Time-resolved energy distribution of the electron emission from the plasma of a micropinch discharge

M. A. Gulin, A. N. Dolgov, N. N. Kirichenko, and A. S. Savelov

Moscow Engineering Physics Institute
(Submitted 5 October 1994)
Zh. Éksp. Teor. Fiz. **108**, 1309–1317 (October 1995)

The time dependence of the electron emission from the plasma of a micropinch discharge has been studied. Electrons with energies >25 keV emitted in the axial direction and x radiation with photon energies >2 keV have been detected with nanosecond time resolution using a multichannel system of scintillators. In order to distinguish the "x-ray" and "electron" signals a magnetic barrier was placed in one of the detection channels. Comparison of the ratio of the electron signal amplitudes from two detectors located behind aluminum filters of thickness 6 and 14 μm with a ratio calculated in accordance with a one-temperature model of the particle energy spectrum permitted two groups of emitted electrons to be identified: one was characterized by an effective temperature $kT_e<8$ keV and the other by a temperature $kT_e>30$ keV. The occurrence of the second group is not directly related to the process by which the dense pinch is formed. © *1995 American Institute of Physics.*

1. INTRODUCTION

Plasma studies of dense Z-pinches have continued owing to both the purely scientific interest in certain physical phenomena, mainly the growth of instabilities in the current-carrying plasma and the associated particle acceleration in high-current pinch discharges, and in connection with the possible applications of micropinch discharges, primarily as high-power x-ray sources.

In order to convert the electrical energy efficiently into short-wavelength radiation it is necessary to achieve pinches with high mass densities close to the time of maximum current, which requires that the balance between magnetic and gas kinetic pressures be maintained in the preceding stage.

The number of current carriers in the transverse cross section of a plasma column decreases and their average velocity increases when the plasma is compressed in the constricted region. This leads to the growth of kinetic instabilities and causes the particle velocity distribution to depart from its equilibrium form. Although the number of superthermal particles is usually relatively small, their contribution to the plasma pressure may be significant or even dominant. It is of prime importance to include the contribution of the superthermal electrons, since the rate of change of the electron distribution function is greater than that for the plasma ions. In order to include the superthermal component we must write the gas kinetic pressure as

$$P=n_{epi}\langle W\rangle+(n_{epi}+n_{th})kT_e+\frac{n_{th}kT_i}{Z_i}, \tag{1}$$

where

$$\langle W\rangle=m_e\int\frac{(f_b-f_m)(v_x^2+v_y^2)}{2n_{epi}}\,dx\,dy\,dz,$$

and f_b is the nonequilibrium distribution function, f_m is a Maxwellian distribution function, m_e is the electron mass, n_{epi} is the density of the superthermal electrons, n_{th} is the density of the thermalized electrons, T_e and T_i are the electron and ion temperatures, and Z_i is the mean charge state in the plasma. Consequently, the Bennett pinch condition for the quasisteady compressed state must be modified as follows:

$$I^2=\frac{8\pi}{\mu_0}\left[N_{epi}\langle W\rangle+(N_{epi}+N_{th})kT_e+\frac{N_{th}kT_i}{Z_i}\right], \tag{2}$$

where I is the discharge current, $N=n\pi R^2$ is the particle line density, and R is the pinch radius. If the mean energy $\langle W\rangle$ of superthermal electrons in the plane transverse to the discharge axis (the z axis in our notation) increases faster than R^2 in the discharge process, then pinching cannot occur.

The fastest mechanism for heating up the electrons and, most importantly, the highest-energy electron component is probably anomalous resistivity, which partly shuts off the conduction current [the process by which the anomalous resistivity develops takes $\lesssim 10^{-12}$ s (Ref. 1) and the micropinch lifetime is $\sim 10^{-10}$ s (Ref. 2)] and causes a potential spike to appear on the boundary of the constricted region, which reaches values $\sim 10^5$–10^6 V. Because the electrons are magnetized they cannot be accelerated directly by the electric field that develops, but as they drift along the axis they are able to gain energy in the electric field.

The relationship between the micropinch dynamics and the development of the accelerating processes in the plasma is still not completely resolved. In the present work we have studied the behavior in time of the electron emission from the plasma of a micropinch discharge.

2. EXPERIMENTAL PROCEDURE

The design of the discharge device (a low-inductance vacuum spark) and a schematic of the experiment are shown in Fig. 1. The discharge was struck in the vacuum chamber in the vapor of the electrode material. The anode (conical) and cathode (a flat ring) were made of iron. The discharge current reached a maximum value of $I_m\simeq 150$ kA in a time $T/4\simeq 20$ μs.

 1063-7761/95/100719-05$10.00

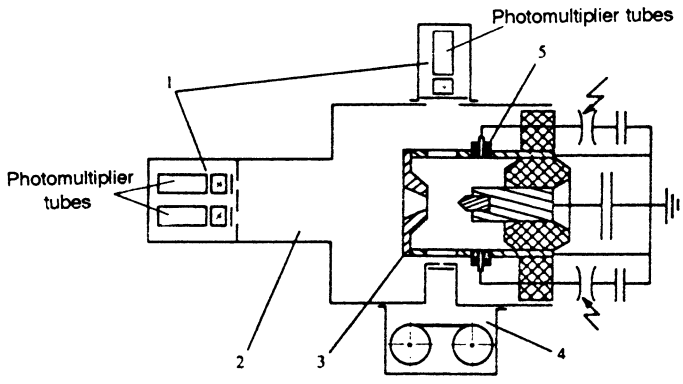

FIG. 1. Design of the discharge apparatus and schematic of the experiment: *1*—scintillation detector; *2*—vacuum chamber; *3*—electrode; *4*—pinhole camera; *5*—triggering device.

Three identical scintillation detectors were located at a distance of 1 m from the electrodes in the axial direction. The plastic scintillators had a time resolution ~2 ns, allowing efficient detection of x radiation and fast electrons with a resolution less than 6 ns. The energy of the detected photons and particles was limited with aluminum filters of thickness 6 μm in two of the detection channels and 14 μm in the other. We were also able to place a magnetic barrier (a transverse magnetic field of magnitude ~1 kG extending a distance ~1 cm) in front of any one of the detectors. This was shielded from the other detectors and acted as a filter for electrons with energies up to ~50 keV. A fourth scintillation detector was located 15 cm from the discharge axis in the radial direction behind a beryllium filter of thickness 100 μm. This actually detected only radiation from the discharge. The derivative of the discharge current was measured with a magnetic probe in synchronization with measurements of the vacuum UV using a planar photodiode. All of these signals were displayed on S8-14 two-beam oscilloscopes. To ascertain the state of the discharge we used photographs of the discharge gap made with an x-ray pinhole camera. The diagnostic equipment is summarized in the table.

3. PROCEDURE FOR MEASURING THE EFFECTIVE ELECTRON TEMPERATURE

In order to determine the energy distribution of the electrons emitted from the plasma discharge, we compared the ratio of the signals from the two scintillation detectors located behind aluminum filters of thickness 6 μm and 14 μm with the calculated ratio of the doses in a scintillator behind absorbing filters of the same thickness due to an electron flux with an energy distribution corresponding to a one-temperature model:

$$\frac{dN}{dE} \propto \exp\left(-\frac{E}{kT_e}\right). \tag{3}$$

By comparing the measured and calculated values we determined the effective electron temperature T_e, i.e., the mean kinetic energy of the detected particles.

The dose was calculated as

$$D(T_e,\tilde{S})=\sum_{i=1}^{n}\frac{dN}{dE}(E_i)F(E_i,\tilde{S})\Delta E, \tag{4}$$

where we have written $\Delta E=20kT_e/n$ and E_i [keV]$=20+i\Delta E$; here $F(E_i,\tilde{S})$ is the dose delivered by one electron in the scintillator behind a filter of thickness $\tilde{S}$:

$$F(E_i,\tilde{S})=\int_{\tilde{S}}^{S_{\max}}\Phi(E_i,S)dS, \tag{5}$$

$S_{\max}$ is the maximum penetration depth for an electron with energy E_i in the material of the filter, and $\Phi(E_i,S)$ is the distribution of the dose as a function of the penetration depth S.

In this temperature range 5 keV $<kT_e<30$ keV the calculated error arising from using a discrete spectrum with $n\sim500$ in place of the continuous spectrum was less than 1%.

TABLE I.

Experimetnal procedure	Energy interval for detected photons $h\nu$, keV*	Detected range of electron energies E, keV**
Scintillation detector (Al filter of thickness 6 μm)	>3	>25
Scintillation detector (Al filter of thickness 14 μm)	>4	>40
Scintillation detector (Be filter of thickness 100 μm)	>2	>100
Planar photodiode	>0.01	···
Magnetic (dI/dt) probe	···	···
Pinhole camera (Be filter of thickness 100 μm)	>2	···

*The cutoff energy for the corresponding filter is given.
**The energy is given for a particle whose maximum penetration depth equals the filter thickness.

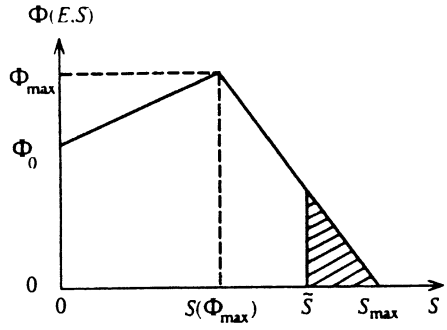

FIG. 2. Model dependence of the dose distribution as a function of depth of penetration.

To find $\Phi(E,S)$ we used the model proposed by Everhart and Hoff[3] for light materials (including aluminum) and carefully calibrated for the energy range 5 keV $<E<60$ keV by comparison with experimental data and the results of Monte Carlo calculations:

$$\Phi(E,S)=\frac{E}{R_G}\lambda(y), \tag{6}$$

$$\lambda(y)=0.60+6.21y-12.40y^2+5.69y^3, \tag{7}$$

$$R_G=0.004\ E^{1.75}, \tag{8}$$

where $y=S/R_G$, $[S]=\text{mg/cm}^2$, $[R_G]=\text{mg/cm}^2$, and $[E]=\text{keV}$.

To find the error resulting from the deviation of this model from the actual dose as a function of depth, we carried out the same calculations for the simplified function $\Phi(E,S)$ shown in Fig. 2. The parameters Φ_0, $S(\Phi_{\max})$, and $S_{\max}$ were defined as follows:

$$\Phi_0=78.5\,\frac{Z}{AE}\ln\frac{1.66E}{1.15\cdot10^{-2}Z}, \tag{9}$$

$$S(\Phi_{\max})=0.01E^{1.43}, \tag{10}$$

$$S_{\max}=2S(\Phi_{\max}), \tag{11}$$

where Z and A are the atomic number and atomic weight of the filter element, and $[S]=\text{mg/cm}^2$, $[E]=\text{keV}$, and $[\Phi]=\text{keV}\cdot\text{cm}^2/\text{mg}$. The quantity $\Phi_{\max}$ was evaluated from the normalization with respect to energy and a single incident electron:

$$E=\int_0^{S_{\max}}\Phi(E,S)\ dS. \tag{12}$$

Equations (9) and (10) were taken from Ref. 4; Eq. (11) was chosen on the basis of the qualitative shape of the function $\Phi(E,S)$ calculated by means of the Monte Carlo method for elements with low Z and energy $E=60$ keV (Ref. 4).

The results of calculating the ratio of the doses behind the aluminum filters of thickness 6 and 14 μm (1.67 and 3.78 mg/cm^2) are shown in Fig. 3.

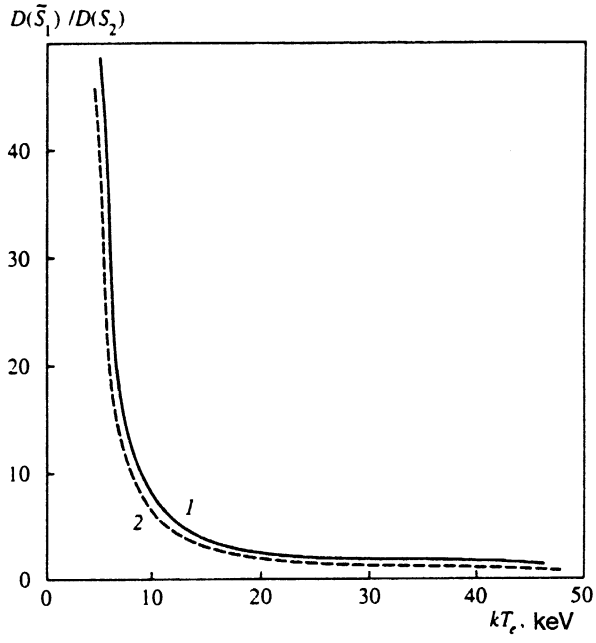

FIG. 3. Calculated relative magnitude of the signals from the two scintillation detectors as a function of the effective temperature of the measured electrons (the magnitude of the signal is assumed proportional to the dose adsorbed in a scintillator): *1*—calculated following Ref. 5; *2*—calculated using the simplified model.

4. EXPERIMENTAL RESULTS

The nature of the signal from the planar photodiode (Fig. 4) shows that based on the pinhole camera pictures before the micropinch formed the plasma pinched effectively only in the first half-period of the discharge current, close to the time at which the current reaches its maximum value. The oscilloscope trace from the magnetic probe (Fig. 5) exhibits a sharp drop, the well-known "singularity," indicating a rapid change in the current flow in the discharge plasma, namely, a decrease in the value of the current. The detector located on a radius (with a beryllium filter of thickness 100 μm) also detected a radiation pulse only in the first half-period of the discharge at the time the singularity occurred.

The signal from the detector on the discharge axis with an aluminum filter of thickness 6 μm is quite complicated. It appeared in the first half-period of the discharge simultaneously with the singularity, with the rise time of the first pulse usually considerably shorter than its width ~1 μs. Behind the first pulse a second one appeared, lasting somewhat longer (~10 μs); the maximum usually occurred about 4–6 μs after the start of the first pulse. The second pulse in the detector channel was not accompanied by spikes in the dI/dt signal of a magnetic probe. When the magnetic barrier was in place in front of the second detector no pulse appeared, while the first pulse generally became somewhat shorter ($\sim$100–200 ns). Near the second maximum of the current another short pulse (100–200 ns) occurred in approximately half the discharges, with a shape which was almost independent of the presence of the magnetic barrier.

As for the signal coming from the detector with the

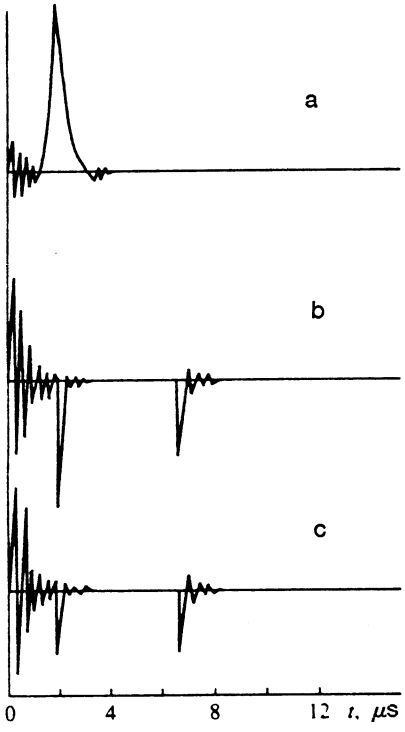

FIG. 4. Oscilloscope traces: a—from the photodiode; b, c—from the scintillation detectors located on the axis behind Al filters of thickness 6 and 14 μm respectively when a magnetic barrier is present.

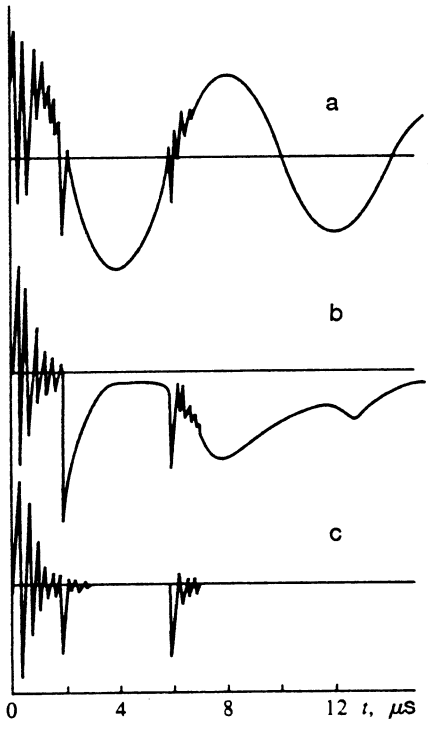

FIG. 5. Oscilloscope traces: a—from the magnetic probe; b, c—from the scintillation detectors located on the axis behind Al filters of thickness 6 and 14 μm respectively, with no magnetic barrier.

thicker Al filter (14 μm), also located on the system axis, it has the form of relatively short pulses of length ~100–200 ns. The first of these appeared at the same time as the singularity in the first half-period of the discharge. The second pulse was not detected in every discharge. But when it was detected it occurred at the same time as the corresponding second pulse in the "soft" detector channel, which was also the second in the sequence (so that the relatively long (~10 μs) pulse referred to a little bit earlier as the "second" in this case is actually the third), and is accompanied by high-frequency oscillations in the magnetic probe channel. Analysis of several dozen oscilloscope traces provides assurance that nothing resembling the spike in the first half-period of the discharge is observed here. It is likely that the observed oscillations of the magnetic field are due to waves which are excited, and not to pinching of the plasma discharge. The presence of the magnetic barrier does not change the nature of the signal.

The ratio of the signal amplitudes which appear simultaneously in the two detector channels (with aluminum filters of thickness 6 and 14 μm) is equal to $I_s/I_h \simeq 1-2$. When no pulse is observed in the second channel (the limitation is the amount of background) the calculated ratio of the signal amplitudes is $I_s/I_h < 0.1$.

5. DISCUSSION OF RESULTS

The signal from the detectors located on the system axis results from measuring the x-ray and fast electron fluxes. Comparison of these signals with that in the photodiode channel and with the radial detector, along with the pinhole camera pictures, shows that close to the time at which the discharge current attains its maximum value in the first half-period a micropinch develops in the plasma discharge. This is the source of the x radiation and the electron flux propagating toward the external electrode. Note that the direction in which the electrons move is the same as that of the current flow, i.e., opposite that in which the electrons drift under the influence of the external electric field applied to the discharge. Measurements previously made of the interelectrode potential drop using a capacitive voltage divider showed that no only do the magnitude and direction of the current vary in the discharge, so also doe the magnitude of the potential and the relative polarity of the electrodes, and with the same period. The difference is that the oscilloscope trace from the voltage divider has little resemblance to a sine wave, e.g., at the time of maximum current a voltage spike is observed (regardless of whether a spike appears on the dI/dt oscilloscope trace).

Two groups of electrons can be distinguished. One reaches the detector almost simultaneously with the radiation, e.g., as a result of diamagnetic drift within the plasma column. Despite the excellent time resolution of the detection system and the considerable propagation distance, we were unable to distinguish the time of arrival of the x-ray pulse and the electron flux because the particle drift time over this distance is less than the width of the x-ray pulse, ~100 ns (Ref. 5; the drift time of 100 ns corresponds to an electron energy 0.25 keV). The second group probably reaches the detector as a component of the plasma flux emitted from the region where the micropinch forms. This is

because of the protracted signal from the scintillation detector behind the Al filter of thickness 6 μm. Studies previously performed show that the energy spectrum of the ions emitted from the region where the micropinch forms extend over the range 1–50 keV, which for this propagation distance corresponds to a drift time for the ions or plasma columns of 2.5–17 μs. From the propagation time we can estimate the drift velocity of this plasma; for the central part of the clump it is $\approx 2 \cdot 10^7$ cm/s, which corresponds to an energy for the iron ions which make up its ionic component of $\approx$10 keV. Such values agree well with the results of calculations[6] for the breakdown stage of the micropinch plasma and with previously obtained data on direct measurement of the ion fluxes from a micropinch discharge.[7]

The calculated relative intensity of the flux of x-ray bremsstrahlung emitted by a plasma with $kT_e = 1-2$ keV, the typical temperature of the micropinch, is equal to 1.5–3 after passing through aluminum filters of thickness 6 and 14 μm. Under the present experimental conditions the results of the measurements cannot be affected by line and photorecombination radiation in the micropinch. The minimum time resolution of the apparatus we used is approximately two orders of magnitude greater than the lifetime of the micropinch itself. During the latter time photorecombination radiation and emission in the lines of the K-spectrum of iron ions in different ionization states should dominate in the 6.3–7 keV spectral range. The detectors were almost totally screened by the filters from radiation in the L-shell portion of the spectrum. The validity of treating the observed emission mainly as bremsstrahlung was confirmed in calibration experiments using Ross filters.[5]

The electron fluxes which appear in the discharge plasma in connection with the formation of the micropinch were not detected with the more restrictive filter, or more precisely we found $I_s / I_h < 0.1$ at these times. An estimate of the effective electric temperature in this case yields $kT_e < 8$ keV, which also agrees with the calculations of Ref. 6.

As for the fast electrons measured only in the second half-period of the discharge, their effective temperature is calculated to be $kT_e > 30$ keV. The origin of this group of electrons is unrelated to the process by which the dense pitch forms; it was determined previously[8] by studying the spectral composition of the x radiation from the micropinch discharge. The mechanisms by which it is generated is probably the same as in classical Z pinches. We were unable to reliably identify electrons of this group during the firs half period of the discharge, although data about the time dependence of the characteristic radiation from the electrode materials, radiation with $h\nu > 100$ keV, and radiation from multicharged ions (e.g., heliumlike) obtained in Ref. 9 implies that electrons with a high effective temperature may be produced in the plasma column of the discharge when the micropinch forms.

6. CONCLUSION

We have measured two groups of hot electrons emitted from the plasma of a low-inductance vacuum spark. The first group appears as a result of plasma heating during the growth of the sausage instability and the formation and subsequent collapse of the micropinch; the effective electron temperature is $kT_e < 8$ keV. The electron flux is primarily in the direction opposite that of the current drift. Part of the electrons represents a component of the plasma flowing out of the micropinch region.

The second group is unrelated to the process by which the micropinch develops in the discharge; its effective electron temperature is $kT_e > 30$ keV. The direction in which this group propagates is the same as that of the current drift.

These studies were carried out with support from the Russian Fund for Fundamental Research (Grant No. 95-02-050790).

[1] S. M. Zakharov, G. V. Ivanenkov, A. A. Kolomenskiĭ, S. A. Pikus, and A. I. Samokhin, Fiz. Plasma **9**, 469 (1983) [Sov. J. Plasma Phys. **9**, 271 (1983)].
[2] E. V. Aglitskiĭ, P. S. Antsiferov, and A. M. Panin, Fiz. Plazmy **11**, 275 (1985) [Sov. J. Plasma Phys. **11**, 159 (1985)].
[3] T. E. Everhart and P. H. Hoff, J. Appl. Phys. **42**, 5837 (1971).
[4] I. Brody and G. Maret, *Physical Basis of Microtechnology*, A. V. Shal'nov, ed. [Russian translation], Mir, Moscow (1965).
[5] V. V. Averkiev, A. N. Dolgov, V. K. Lyapidievskiĭ, A. S. Savelov, and G. Kh. Salakhutdnov, Fiz. Plazmy **18**, 724 (1992) [Sov. J. Plasma Phys. **18**, 374 (1993)].
[6] V. V. Vikhrev, V. V. Ivanov, and K. N. Koshelev, Fiz. Plazmy **8**, 1211 (1982) [Sov. J. Plasma Phys. **8**, 681 (1982)].
[7] A. A. Gorbunov, M. A. Gulin, A. N. Dolgov, O. V. Nikolaev, and A. G. Savelov, Preprint No. 024-88, Moscow Engineering Physics Institute, Moscow (1988).
[8] A. N. Dolgov, N. N. Kirichenko, V. K. Lyapidievskiĭ, A. S. Savelov, and G. Kh. Salakhutinov, Fiz. Plazmy **19**, 97 (1993) [Sov. J. Plasma Phys. **19**, 80 (1993)].
[9] V. A. Veretennikov, A. I. Isakov, O. N. Krokhin, O. G. Semenov, and Y. V. Sidel'nikov, Preprint No. 59, Lebedev Physical Institute, Moscow (1983)

Translated by David L. Book